

Article

# Watershed Hydrological Response to Combined Land Use/Land Cover and Climate Change in Highland Ethiopia: Finchaa Catchment

Wakjira Takala Dibaba <sup>1,2,\*</sup>, Tamene Adugna Demissie <sup>2</sup> and Konrad Miegel <sup>1</sup>

<sup>1</sup> Hydrology and Applied Meteorology Department, Faculty of Agricultural and Environmental Sciences, University of Rostock, Satower Str. 48, 18059 Rostock, Germany; konrad.miegel@uni-rostock.de

<sup>2</sup> Faculty of Civil and Environmental Engineering, Jimma University, Jimma 378, Ethiopia; tamene.adugna@ju.edu.et

\* Correspondence: wakjira.dibaba@uni-rostock.de

Received: 20 May 2020; Accepted: 21 June 2020; Published: 24 June 2020



**Abstract:** Land use/land cover (LULC) and climate change affect the availability of water resources by altering the magnitude of surface runoff, aquifer recharge, and river flows. The evaluation helps to identify the level of water resources exposure to the changes that could help to plan for potential adaptive capacity. In this research, Cellular Automata (CA)-Markov in IDRISI software was used to predict the future LULC scenarios and the ensemble mean of four regional climate models (RCMs) in the coordinated regional climate downscaling experiment (CORDEX)-Africa was used for the future climate scenarios. Distribution mapping was used to bias correct the RCMs outputs, with respect to the observed precipitation and temperature. Then, the Soil and Water Assessment Tool (SWAT) model was used to evaluate the watershed hydrological responses of the catchment under separate, and combined, LULC and climate change. The result shows the ensemble mean of the four RCMs reported precipitation decline and increase in future temperature under both representative concentration pathways (RCP4.5 and RCP8.5). The increases in both maximum and minimum temperatures are higher for higher emission scenarios showing that RCP8.5 projection is warmer than RCP4.5. The changes in LULC brings an increase in surface runoff and water yield and a decline in groundwater, while the projected climate change shows a decrease in surface runoff, groundwater and water yield. The combined study of LULC and climate change shows that the effect of the combined scenario is similar to that of climate change only scenario. The overall decline of annual flow is due to the decline in the seasonal flows under combined scenarios. This could bring the reduced availability of water for crop production, which will be a chronic issue of subsistence agriculture. The possibility of surface water and groundwater reduction could also affect the availability of water resources in the catchment and further aggravate water stress in the downstream. The highly rising demands of water, owing to socio-economic progress, population growth and high demand for irrigation water downstream, in addition to the variability temperature and evaporation demands, amplify prolonged water scarcity. Consequently, strong land-use planning and climate-resilient water management policies will be indispensable to manage the risks.

**Keywords:** climate; flow; hydrology; runoff; RCP; water resources

## 1. Introduction

Our world is functioning at a mixture of complex systems interacting at a variety of spatial and temporal scales in which both the natural and human factors are thoroughly intertwined. The strong relationship between land use, water and climate from these systems has contributed to prominent concern to the basic planet characteristics and process. The productivity of land, biodiversity, aridity

and drought, desertification, land degradation, climate change and hydrological process are some of the process [1–6]. Furthermore, the conflicting interactions between the past and present land use, socio-economy and ecological priorities exposed the earth to face land degradation, which leads to desertification that reduces the potential productivity of the land [5].

Land use/land cover change (LULCC) and climate change, triggered by the global and regional economic development, will alter the availability and competition for water [7]. Rapid population growth and increasing demands for food and water resources, combined with high rainfall variability and frequent hydrological extremes further undermine the environment by altering the availability of different biophysical resources. Moreover, the expansion and intensification of agricultural lands, development of urban areas, as well as the need to extract wood products and fire fuel are increasing to meet the needs of an increasing population [2,8]. When the LULCC aggregates globally, key aspects of the earth's system functioning will be affected as LULCC is not only a local environmental issue, but is also becoming a force of global importance [9,10]. Climate change has the potential to impose extra pressure on water availability and accessibility. These changes are expected to produce detrimental environmental effects, thereby increasing interests of its effect on the hydrological process.

Factors like demography, institutions, technology, biophysical, national and local policies and macroeconomic activities result in an extensive alteration of LULCC which affect the hydrological systems both, at the basin and regional scales [2,11,12]. Further, LULCCs are the dominant drivers for the links and further associating terrestrial and atmospheric components of the hydrological cycle [13], and are related to the amount of water through a hydrological process [14]. On the other hand, climate change affects the hydrological cycle by changing runoff over watersheds, disturbing the transformation and transport characteristics of the catchment hydrology [15]. Therefore, the rapid changes in land use/land cover (LULC), coupled with climate change, might lead to the increased hydrological impacts of watersheds by altering the magnitude of the hydrological process [16–18]. However, the exploration and understanding of how LULCC and climate changes continue to interact and disturb the catchment hydrology vary from global to regional and regional to local scale. Therefore, scientific investigations to understand the interactions between LULCC and climate change, and their effect, is required to manage the water resource and environment in the face of future changes. Further, new and updated insights on water and land conditions, as well as management options can facilitate more proactive approaches to maintain the water resources and land health through reversing degradation risk.

Modelling LULCC helps to detect where the change has, or will potentially, occur. Furthermore, the analysis of changes at different spatio-temporal scales, and the prediction of its future scenario, helps reveals the process and mechanisms of global and regional changes [19,20]. Although the factors that contributed to the changes can be assessed, factors in the prediction of LULC are more probabilistic. In this regard, much is needed to estimate the LULCCs over the past, and predict the future scenario of these changes. From the variety of techniques that have been used for LULCC detection using remote sensing products, cellular and agent-based models are the most commonly used methods [21]. Cellular Automata (CA) alone can predict spatial distribution, but not temporal changes, whereas Markov can predict dynamic changes of landscape pattern but unable to predict spatial patterns of landscape change. For these reasons, many researchers have applied the mixed model, based on the two methods in different places. Combining CA-Markov integrates the advantages of CA with Markov analysis to predict the long term future land use trends [19–23].

In the past, only a few studies explicitly acknowledged the combined effect of LULCC and climate change in different parts of the World [15,24,25]. However, it is becoming one among the utmost prevalent areas of research [22,26–30]. These studies suggest that the hydrological responses of catchments to LULCC vary with the climate and physical characteristics of the catchments. Further, Qi et al. [24] showed that future hydrological changes and LULCC are expected to be site-specific, and that climate variability is an important factor for controlling the basin hydrological process. Combalicer and Im [31] showed that climate variability leads to a direct impact on hydrology on a watershed. However, the response of future climate conditions may vary depending on the LULCC.

The LULCC studies in different parts of Ethiopia revealed LULCC processes are intense in the highland parts, driving unprecedented changes at different scales [2,32–35]. However, the extent of changes in LULC varied markedly. Most of the land use/land cover studies addressed only the human-managed systems of resource degradation, brought by the reduction of the cover of natural vegetation, and its conversion to other LULC types. Likewise, climate change studies in Ethiopia on future seasonal and annual hydrological variables have shown increasing stresses of water resources availability [11,36–40]. However, different studies have projected climate changes with different strengths of influence. For example, Shiferaw et al. [39] on Ilala watershed reported an increasing temperature. However, rainfall does not show significant change. Decreasing precipitation and the increasing temperature are reported in the Rift valley of Ethiopia [40]. Elshamy et al. [41] on impacts of climate change on the Blue Nile basin using multiple GCMs reported that most models showed a reduction of the annual precipitation, while some models proving the opposite. Overall, most of the studies on LULCC neglected the climate change effects and vice versa. Their interaction is not well-understood as they are highly interrelated and the knowledge on scales, relevant to the local stakeholders, farmers and decision-makers on the effect of LULCC and climate change is still limited. An understanding of the values and impacts of land, water and climate management, how and where to target interventions are required to achieve a healthy ecosystem, land use and climate change mitigations.

Even though the availability of land and water in Africa is highest in the world, some areas of sub-Saharan Africa are seriously threatened through overuse because of the ever-increasing needs of the growing population and inappropriate land management practices [42]. Further, changes in hydrology and water resources, due to climate and land modification, warrant intensive attention in East Africa's key water towers, Blue Nile River as the massively dependent population are on rain-fed agriculture [43]. In particular, the upper Blue Nile, the predominant sources of Blue Nile is facing intensive and extensive effects of LULCC [44–46] and climate changes [38,43,47,48]. Fluctuations of seasonal and annual flows, and decline in flows in some watersheds are mainly driven by erratic and unpredicted changes in climate variables and undesirable changes in LULCC [49,50]. Finchaa catchment, a part of upper Blue Nile is among the watersheds facing the challenges. Rapid population growth, with the expansion of commercial farm and cultivation lands, coupled with rapid urban expansion in the catchment, have brought unprecedented LULCC [2,44,51]. Furthermore, the high rising demands of water in Finchaa catchment, due to the socio-economic progress and high demand for irrigation water for sugarcane cultivation, are increasing pressure on water resources of the catchment. The studies in the catchment that quantified the historical LULCC [44,46] and climate change studies [48,52] showed that the water resources in Finchaa catchment are highly sensitive to changes in LULCC and climate.

The fact that the country's relatively abundant water resources have played a minimal role in the Nation's economic development. The Ethiopian government intends to place a priority on water resource development as an essential strategy for economic and social development of the country [53]. The need for national economic development and the relevance of water resources for the country's socio-economic development for the promotion of sustainable development, relies on the management of water resources, linked with the ongoing and planned development projects.

Consequently, studies that consider both the isolated and combined effects of LULCC and climate changes of the specific area are required at regional and local scales as drivers of changes, not limited to global and regional levels, but also local specific. Specifically, this research has been initiated to investigate the watershed hydrological response to the LULCC and climate changes. Integrated approaches of CA-Markov analysis for LULC prediction and ensemble mean of four regional climate models (RCMs) in the coordinated regional climate downscaling experiment (CORDEX)-Africa were used for the future climate change scenarios. Then, the Soil and Water Assessment Tool (SWAT) hydrological modelling was used for the evaluation of isolated and combined LULCC and climate change impacts. Specifically, this study was aimed at (1) assessing and modelling the LULCC scenarios

and its impacts, (2) assessing and modelling the climate change and its impacts, (3) examining the combined effects of LULCC and climate change, and (4) exploring how the water resources are sensitive to the changes. The findings of these studies provide plausible insights on the vulnerability of the Finchaa catchment to LULCC and climate change.

## 2. Materials and Methods

### 2.1. Study Area

The study was conducted in the upper Blue Nile Basin, Finchaa sub-basin in Oromia Regional State, Ethiopia. Finchaa sub-basin lies in 9°10' to 10°00' North latitude and 37°00' and 37°40' East longitude covering 3781 km<sup>2</sup> areas. The catchment is characterized by high topographic relief, with elevation ranging from 851 to 3213 m above sea level. The area has large upstream water potential sites, intensive irrigable downstream lands, and high hydropower potential. The sub-basin contains three watersheds; Fincha, Amerti and Neshe [2]. The detail study area description is shown in Figure 1.

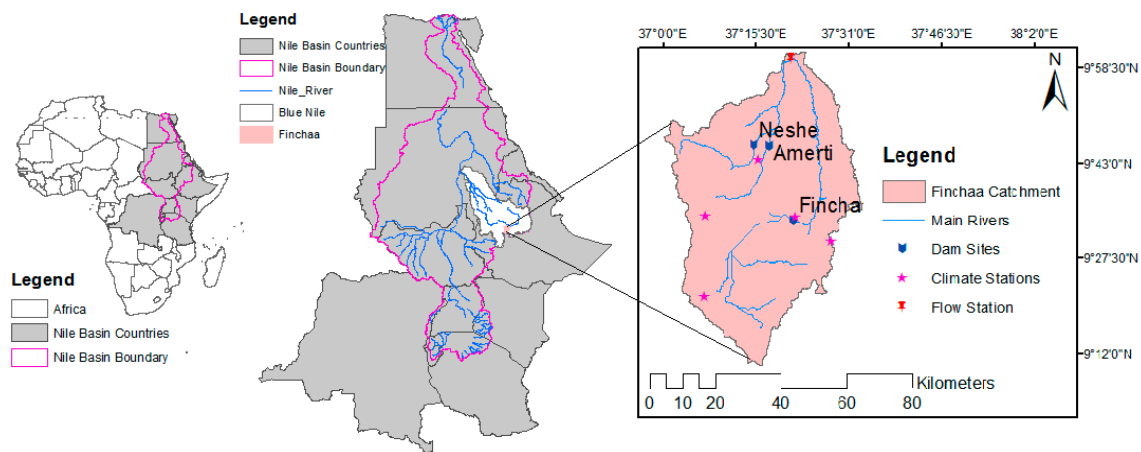


Figure 1. Map of the study areas.

The annual rainfall of Finchaa catchment ranges from 1367 mm to 1842 mm, with the lower rainfall occurring in the northern lowlands, and the higher rainfall is greater than 1500 mm occurring in the southern and western highlands of the sub-basin. June to September is the main rainy season of the catchment, with an average annual rainfall of 1604 mm and a peak occurring between July to August [54]. The mean monthly temperature of the catchment varies between 15.50 °C to 18.62 °C.

Agro ecologically, Finchaa sub-basin is characterized by tepid to cool sub-humid mid highlands in the north-western, moist mid highlands in the south-eastern, and hot to warm moist lowlands in the north-eastern parts of the catchment.

### 2.2. Data Sources and Methodology

#### 2.2.1. Data

A 30 × 30 m resolution of the Digital Elevation Model (DEM) obtained from the United States Geological Survey (USGS) at <https://earthexplorer.usgs.gov/> was used to delineate the watershed of the study area. Moreover, it is used for slope classification, which was the basis for the Hydrological Response Unit (HRU) generation. The areas of different land slope classes as shown in Figure 2 shows that the majority of the land is 31.57%, and is found with a slope greater than 15%, 24.13%, are present between 0% and 4%, 21.77% between 4% and 8% and the remaining 22.53% between 8% and 15%, showing a variation of higher topographic in Finchaa catchment.

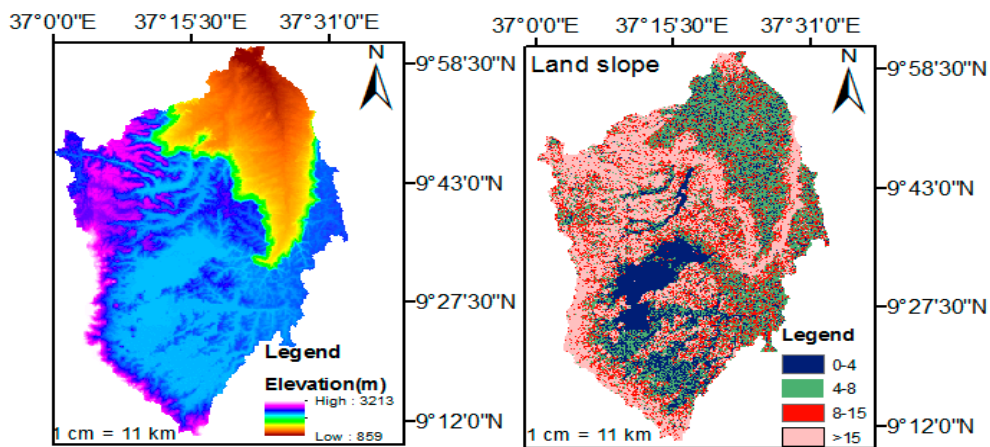


Figure 2. Elevation and slope maps of Finchaa catchment.

The SWAT model requires a basic physic-chemical property of the soil types. In this study, the major soil types were collected from the Ministry of Water, Irrigation and Electricity (MoWIE), a 250 m resolution of soil grids accessed at [https://soilgrids.org/#/?layer=TAXNWRB\\_250m&vector=1](https://soilgrids.org/#/?layer=TAXNWRB_250m&vector=1), the world digital soil map at <http://www.fao.org/geonetwork/srv/en/metadata.show?id=14116> and FAO soil [55]. The soil classification used in this study is based on the FAO classification system and customized in the way the SWAT model requires, as shown in Figure 3b. Ten different soil types were identified, as shown by Figure 3a. The most dominant soil type of the catchment is Haplic Alisols covering 42.8% areas of the land. The higher areas of the valley are dominated by haplic Arenosols (7.8%), valley areas are dominantly covered with Eutric Cambisols (13.63%), the upstream reach of Fincha reservoir is covered with marsh (9.1%) and Rhodic Nitisols (13.18%) are found around Nashe reservoir.

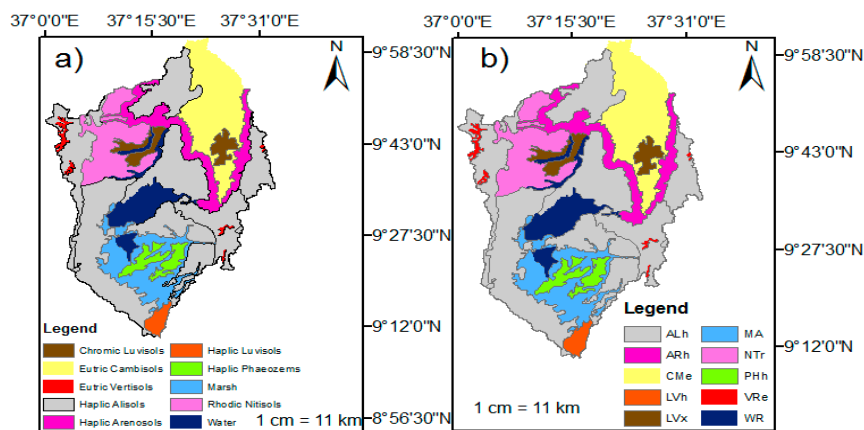


Figure 3. Soil maps of Finchaa catchment (a) soil names; (b) Soil SWAT code.

The daily climate data required by the SWAT model was obtained from the National Meteorological Service Agency of Ethiopia. Based on the record length and the quality of data (less missed data values), only five stations located inside the study catchment were used in this study. The stations that only record rainfall, and stations with many missing values, were not used. Further, for selected stations, the missing data values have been filled with the Inverse Distance Weighting (IDW) method. The consistency of the data was also checked by a double mass curve and found to be consistent. Daily streamflow data for the years 1988–2008 required for SWAT model evaluation was obtained from the MoWIE, hydrology department.

### 2.2.2. Impact Assessment Framework

The hydrological responses of Finchaa catchment to the impacts of LULCC and climate change were investigated for two future periods of 2021–2050 and 2051–2080. The baseline period consists of the years 1986–2015. Three simulation scenarios were developed for the independent and combined effects of the LULCC and climate change. The first scenario (S1) considers only LULCC, the second scenario (S2) considers only climate change and the third scenario (S3) considers both LULCC and climate change (the combination of the two). Details of the scenarios are depicted in Table 1.

**Table 1.** Detail land use/land cover and climate change scenarios.

Scenarios	Description
S1	Only LULCC—land use maps of 2017, 2036 and 2055 with baseline climate data from 1986 to 2015 were used.
S2	Only a climate change-baseline map of land use 2017 was used with a climate scenario of 1986–2015, 2021–2050 and 2051–2080.
S3	Combined LULCC and climate change- land use maps of 2017, 2036 and 2055 were used with 1986–2015, 2021–2050 and 2051–2080 climate data, respectively.

### 2.2.3. Land Use/Land Cover Change Modelling

CA-Markov model integrates the advantage of CA theory with the temporal forecasting ability of the Markov model. Consequently, the CA-Markov model outperforms the other methods of modelling the temporal and spatial dimensions of LULCCs [20,56]. The approach of CA-Markov in IDRISI involves two techniques: Markov chain analysis and CA. The procedures of projecting LULCCs with CA-Markov outlined by Pan et al. [22] in the framework of IDRISI software was used in this study. The procedure involves three steps: calculating the transition matrix, creating suitability maps and prediction of the LULC map. The LULC transition matrix was developed by the Markov chain model in IDRISI. Then, the suitability maps of the potential driving factors of the LULC translations are developed for each LULC classes with the multi-criteria evaluation (MCE). Factors such as road proximity, water body proximity, elevation, slope, and urban and built areas were used as criteria to generate suitability maps. Finally, the prediction of the LULC maps are done based on the transition matrix and suitability maps.

For the LULCC analysis, three maps of LULC map for 1987, 2002 and 2017 developed by Dibaba et al. [2] were used. Dibaba et al. [2] used Landsat images from the thematic mapper (TM) for 1987 and 2002, and Landsat 8 operational land imager (OLI) for 2017 to evaluate the spatio-temporal LULCC in Finchaa catchment. The land use maps of 2002 and 2017 were taken as a baseline map and CA-Markov in IDRISI software was used to predict future land use maps of LULC2036 and LULC2055.

Any model prediction requires model calibration and validation. Then, the usefulness of the model output is dependent on the validation results of the model. The performance of the CA-Markov model in predicting the land use maps was assessed using Kappa coefficients calculated by Equation (1) [22,57]. In this study, the LULC maps of 1987 and 2002 were used to simulate the 2017 LULC map. Then, the simulated LULC map of 2017 was compared with the observed 2017 LULC map using the Kappa index:

$$\text{Kappa} = \frac{P_o - P_c}{1 - P_c} \quad (1)$$

In the above equation,  $P_o$  is the proportion of correctly simulated cells;  $P_c$  is the expected proportion correction by chance between the observed and simulated map. If  $\text{Kappa} \leq 0.5$  shows rare agreement,  $0.5 \leq \text{Kappa} \leq 0.75$  shows a medium level of agreement,  $0.75 \leq \text{Kappa} \leq 1$  shows a high level of agreement and  $\text{Kappa} = 1$  for perfect agreement.

#### 2.2.4. Climate Change Scenarios

After evaluating the performance of six Regional Climate Models (RCMs) in Coordinated Regional Climate Downscaling Experiment (CORDEX) Africa, four RCMs showing a better performance were selected. Detail analysis of the CORDEX evaluation is presented in Dibaba et al. [54]. The study by Dibaba et al. [54] on how well the individual RCMs simulate precipitation and temperature of two Ethiopian highland catchments, including Finchaa, proved that ensemble mean outperforms most of the individual RCMs. A similar study by Gadissa et al. [40] in the central Rift valley basin showed that the ensemble mean of five RCMs have shown better performance than individual RCMs. Using multi-RCMs for climate modelling helps to minimize uncertainties, compared to the use of a single RCMs. However, despite the reasonable performance of the RCMs including the ensemble mean, all RCMs have exhibited noticeable biases. Therefore, corrections to the biases should be done before the climate change impact study.

The RCMs used in this study were: CCLM4-8, HIRHAM5, RACMO22T and RCA4, fed by data of the two representative concentration pathways (RCP) scenarios high emission scenario (RCP8.5) and mid-range mitigation emission (RCP4.5). The years 2021–2050 and 2051–2080 served as future scenario periods and the period from 1986 to 2015 as a historical baseline to evaluate the climate changes. Other weather variables, including solar radiation, relative humidity and wind speed in baseline/historical period were considered in the future scenarios without making any change as the changes in these variables may not have a significant impact in modelling the climate change scenarios on local hydrology [40].

#### 2.2.5. Bias Correction

The climate model data for hydrological modelling (CMhyd) [58], obtained from <https://swat.tamu.edu/software/>, was used to process the precipitation and temperature bias correction. Teutschbein and Seibert [59] have provided a full review of the bias correction techniques. According to Teutschbein and Seibert [59], all the bias correction techniques have improved the simulation of precipitation and temperature. However, there are differences between the correction methods in the daily precipitation series, standard deviations, and percentiles. Based on mean absolute error ranking, distribution mapping was ranked both, for temperature and precipitation corrections.

The distribution mapping (DM) uses a transfer function to adjust the cumulative distribution of estimated data to the cumulative distribution of rain gauges [59]. Luo et al. [60] applied seven precipitation bias correction methods and five methods for temperature. The results showed that distribution mapping reproduces precipitation and temperature very well. A similar study by Zhang et al. [61] compared five bias correction methods, using CMhyd, and found distribution mapping performed best for climate change impact study on streamflow dynamics of two rivers in Northern lake Erie basin, Canada. The study by Geleta and Gobosho [52] used CMhyd for extraction of CORDEX-NetCDF, and bias correction of minimum and maximum temperature to predict climate change-induced temperature changes in Finchaa catchment. The study showed that distribution mapping was better in improving the simulation. Owing to all the above findings, distribution mapping served as a basis for the precipitation and temperature corrections before using CORDEX-RCMs outputs for a climate impact study.

#### 2.2.6. Hydrological Model

Soil and Water Assessment Tool (SWAT) is a physically-based semi-distributed model that operates on a continuous time scale [62]. SWAT model operates on a daily time step and predicts the impact of land management in large complex watersheds with varying soils, land use and management conditions. Major model components include DEM, weather, hydrology, soil and properties and land management [63]. In SWAT, a watershed is divided into multiple sub-watersheds, which are then further subdivided into Hydrologic Response Units (HRUs) that comprise homogeneous land use,

slope and soil characteristics. The hydrological components in the model are based on the water balance equation [63] given in Equation (1):

$$SW_t = SW_o + \sum_{i=1}^t (R_{day} - Q_{surf} - E_a - W_{seep} - Q_{gw}). \quad (2)$$

where,  $SW_t$  is the final soil water content (mm),  $SW_o$  is the initial water content (mm),  $t$  is the time (days),  $R_{day}$  is the amount of precipitation on day  $i$  (mm),  $Q_{surf}$  is the amount of surface runoff on day  $i$  (mm),  $E_a$  is the amount of evapotranspiration on day  $i$  (mm),  $W_{seep}$  is the amount of water entering the vadose zone from the soil profile on day  $i$  (mm) and  $Q_{gw}$  is the amount of return flow on day  $i$  (mm).

In the SWAT model, the simulation of the hydrological process begins with watershed delineation and generating streamflow networks. With a 30 m resolution DEM, Finchaa watershed is delineated into 25 sub-basins and a multiple HRU was defined with classes of 10% land use, 20% soil and 10% slope. Accordingly, 231 HRUs were created. Then, with the input of weather data from five stations (Fincha, Hareto, Kombolcha, Nashe and Shambu), the SWAT model setup was ready for the first simulation, which was used for model evaluation. Shambu station, consisting of all the climate variables, was considered a weather generator.

Before using the output of the SWAT simulation for analysis, the performance of the model was evaluated for the catchment. Although distributed hydrological models can relate spatial changes of LULCC to the hydrological process simulation, it is difficult to transform many calibrated parameters into time-variant conditions of the future, especially if empirical parameters are used [22]. Therefore, parameters of the SWAT model are calibrated and validated by historical data and were assumed to have the extrapolative ability under future scenarios.

#### 2.2.7. Sensitivity Analysis, Calibration and Validation

Owing to a large number of flow parameters in SWAT, identifying the most sensitive parameters is necessary to improve the calibration of the hydrological model. Through the sensitivity analysis, the most sensitive parameters that strongly influence the flow process will be identified. The Sequential Uncertainty Fitting (SUFI-2) embedded in the SWAT-CUP (Calibration and Uncertainty Program) was used to achieve the sensitivity analysis, calibration and validation [64].

Calibration of the hydrological model is the process of estimating model parameters by comparing the model prediction with the observed data for the same condition [64,65]. Calibrations are very important for parameters that were not measured and are intrinsically heterogeneous and uncertain, as it serves to optimize the unknown model parameters. For model calibrations, rules of parameter regionalization given by Abbaspour et al. [66] was used. Validation is used to test the calibrated model without further parameter adjustments with an independent dataset. Observed streamflow of 1987–2007 was split into a warm-up (1987–1989), calibration period (1990–2000) and validation period (2001–2006).

The fitness of the model simulation with the observed streamflow was expressed by statistics like coefficients of determination ( $R^2$ ), Nash-Sutcliffe efficiency (NSE), percent bias (PBIAS) and the ratio of the root-mean-square error to the standard deviation of measured data (RSR). The model performance ratings were based on the statistics recommended by Moriasi et al. [65] and Ayele et al. [67]  $R^2$  varies between 0 and 1, where higher value shows less error. NSE ranges from negative infinity to 1 (best). PBIAS close to 0 shows best the simulation, a negative value indicates overestimation and a positive value indicates under simulation of the model. RSR varies from zero to a large positive number. The lower RSR shows a better simulation of the model. These statistics are calculated using Equations (2) to (5):

$$R^2 = \frac{\sum_{i=1}^n [(Q_{mi} - \bar{Q}_m)(Q_{si} - \bar{Q}_s)]^2}{\sqrt{\sum_{i=1}^n (Q_{mi} - \bar{Q}_m)^2 \sum_{i=1}^n (Q_{si} - \bar{Q}_s)^2}}; 0 \leq R^2 \leq 1 \quad (3)$$

$$NSE = 1 - \frac{\sum_{i=1}^n (Q_{mi} - Q_{si})^2}{\sum_{i=1}^n (Q_{mi} - \bar{Q}_m)^2}; -\infty \leq NSE \leq 1 \quad (4)$$

$$PBIAS = 100 \left( \frac{\sum_{i=1}^n Q_{mi} - \sum_{i=1}^n Q_{si}}{\sum_{i=1}^n Q_{mi}} \right) \quad (5)$$

$$RSR = \frac{RMSE}{STDevQ_m} = \frac{\sqrt{\sum_{i=1}^n (Q_{mi} - Q_{si})^2}}{\sqrt{\sum_{i=1}^n (Q_m - \bar{Q}_m)^2}} \quad (6)$$

In the above equations,  $Q_m$  is the measured discharge,  $Q_s$  is the simulated discharge,  $\bar{Q}_m$  is the average measured discharge, and  $\bar{Q}_s$  is the average simulated discharge.

The propagation of uncertainties in model outputs in SUFI-2, expressed as the 95% probability distribution, calculated by the 2.5% and 97.5% levels of the cumulative distributions of output variables, is considered as 95PPU [64]. P-factor and R-factor statistics are considered quantifying, the fit between the result expressed as 95PPU and observation. P-factor, the percentage of observations covered by the 95PPU varies from 0 to 1 with the ideal value of 1 while for R-factor, the thickness of the 95PPU optimal value is around 1.

### 3. Results and Discussion

#### 3.1. CA-Markov Model Performance and Land Use/Land Cover Change Projections

The observed LULC1987 and LULC2002 were used to facilitate the simulation of LULC2017 using CA-Markov model. Then, the observed LULC2017 were cross-compared with the simulated LULC2017 to evaluate the performance of the model using the kappa index. Accordingly, the calculated Kappa index is calculated as 0.87. The result reveals a high level of agreement between the simulated and observed LULC2017, showing the CA-Markov model is strong to simulate the future LULC in the study area.

The LULC classes of Finchaa catchment were grouped into eight classes: agriculture, commercial farm, forestland, grazing land, rangeland, urban and built up, swampy and water bodies. From the land use maps of 2002 and 2017, Finchaa catchment was characterized by expansion of intensive agriculture and urbanization resulting in a natural vegetation decline. Commercial farm, urban and built-up and agricultural lands have increased as shown by Table 2. The highest decline in forest land from 2002 to 2017 was dominantly due to the expansion of commercial farms. The expansion in commercial lands was carried out, in order to double the sugar production by increasing the area of sugarcane cultivation.

**Table 2.** Percentage (%) of LULC in Finchaa catchment.

LULC Classes	Past LULC		Predicted LULC	
	2002	2017	2036	2055
Agricultural Land	42.64	53.39	56.78	56.27
Commercial Farm	1.38	5.76	10.04	11.05
Forest Land	17.61	9.01	5.69	4.67
Grazing Land	12.10	9.68	8.89	8.58
Range Land	16.93	12.05	8.17	9.47
Swampy	3.12	2.39	2.29	1.27
Urban and Built-up	0.27	1.60	2.95	3.72
Water Body	5.94	6.12	5.18	4.97

The future prediction of LULC 2036 and LULC 2055 were executed using the 2017 land use map as a base map. The transition matrix and transfer probability matrix were developed according to the

LULC data of 2002 and 2017. The predicted results of 2017–2036, as shown in Table 2 and Figure 4, show agricultural land, commercial farm and urban and built-up areas are increasing, while forestland, grazing lands, rangelands, swampy and water bodies are decreasing. In 2036 to 2055, commercial farms and urban and built-up was predicted to increase continuously. However, the rate of agricultural land and commercial farm expansion is lower compared to the result of the previous prediction. This might be possible due to the limited area of land for the commercial farm expansion, as the farms are based on irrigation. Furthermore, the increase in range land through continuous future conservation works (soil and water conservation works are already started) might contribute to the decline of agricultural expansions. The high rate of urbanization could also contribute to this. The increase of the shrublands due to the planned afforestation could also be another possible reason.

The SWAT model requires the LULC classes to be reclassified in the code that the model recognizes. Accordingly, the LULC classes are defined with their equivalent representative, as shown in Figure 4.

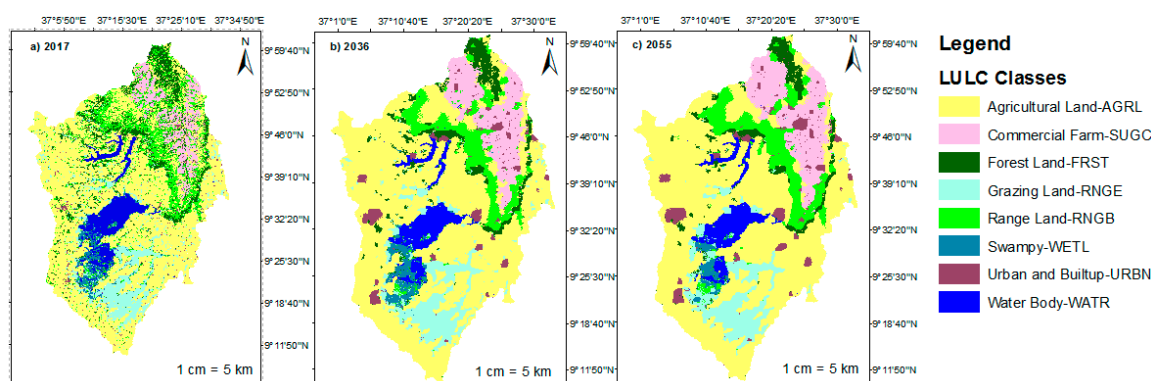


Figure 4. Land use/land cover maps and their SWAT code.

### 3.2. Hydrological Model Performance

#### Sensitivity Analysis, Calibration and Validation

Sensitivity analysis for the simulated streamflow was performed using a daily observed flow to identify the most sensitive parameter with strong influence on model outputs. Initially, parameters related to surface runoff, groundwater, geomorphology, evaporation and soil water were considered and 11 parameters were identified as the most sensitive parameters for calibration. The given ranks are shown in Table 3. The calibration was carried out fitting the model to the streamflow record of 1990–2000. Afterwards, the calibrated values of these 11 parameters were used for further simulations. The parameter ranking was taken from the last iterations of SUFI-2 based on  $t$ -stat and  $p$ -stat. The larger in the absolute value of  $t$ -stat and the smaller the  $p$ -value, the more sensitive is the parameter [64]. As it can be seen from the table, the top three most sensitive parameters are CN2 (moisture condition II curve number), SOL\_AWC (Available water capacity of the soil layer) and RCHRG\_DP (Deep aquifer percolation fraction).

The calibration results on mean monthly flow show that SWAT model is able to capture the observed streamflow with  $R^2$ , NSE, PBIAS and RSR of 0.71, 0.71,  $-1.1$ , and 0.54 respectively. The average monthly flow validation indicates  $R^2$ , NSE, PBIAS and RSR of 0.81, 0.76, 14.3 and 0.49 respectively. This indicates that the performance of the SWAT model in the validation is good enough to simulate the stream flow in the Finchaa catchment. Furthermore,  $p$ -factor and  $R$ -factor statistics showed good agreement with 0.86 and 0.77 during calibration and 0.73, and 0.7 during validation, respectively. Overall, the statistics for goodness fit shows good agreement between the observed and simulated average monthly flow. However, the model is not able to simulate all peak flows well, as shown in Figure 5.

**Table 3.** Sensitivity analysis and calibrated parameters.

Parameter Name	Sensitivity			Calibration	
	t-Stat	p-Value	Sensitivity Rank	Parameter Value Range	Fitted Value
1:r_CN2.mgt	-18.58	0.00	1	±25%	-1.548%
12:r_SOL_AWC (...).sol	-4.79	0.00	2	±25%	4.62%
2:a_RCHRG_DP.gw	-3.40	0.00	3	0–1	0.008
9:v_CH_K2.rte	-2.22	0.03	4	5–130	107.71
4:a_GW_DELAY.gw	-1.79	0.07	5	±10	-4.342
3:v_ALPHA_BF.gw	1.47	0.14	6	0–1	0.449
15:v_SLSUBBSN.hru	-0.83	0.41	7	10–150	71.909
6:a_GW_REVAP.gw	-0.58	0.56	8	±0.036	0.0004
17:v_EPCO.bsn	0.55	0.58	9	0–1	0.421
11:r_SOL_K (...).sol	0.54	0.59	10	±25%	3.75%
13:r_HRU_SLP.hru	-0.46	0.65	11	±0.25	0.138

r-means multiplying initial parameter value by its percent, v-replacement of the initial value of the parameter, a-adding value to initial parameter value.

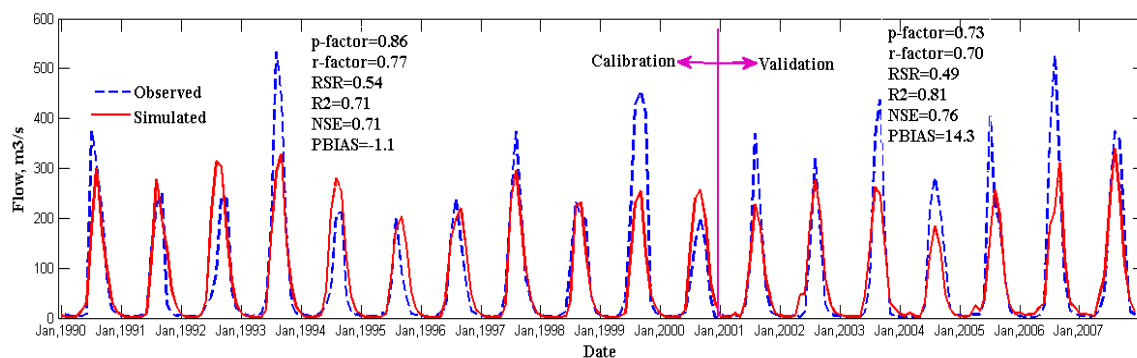


**Figure 5.** Calibration and validation of average monthly streamflow.

### 3.3. Climate Change Projections of the RCMs

To illustrate how each RCMs predicted precipitation and temperature, the projection of individual RCMs and ensemble mean of the RCMs were analyzed. The bias-corrected precipitation, and temperature within distribution mapping for future scenarios, are compared to the baseline data sets (1986–2015). Further, the hydrological responses of the catchment are analyzed by quantifying and comparing the future water balance components (surface runoff, groundwater flow, total water yield and evapotranspiration).

#### 3.3.1. Rainfall

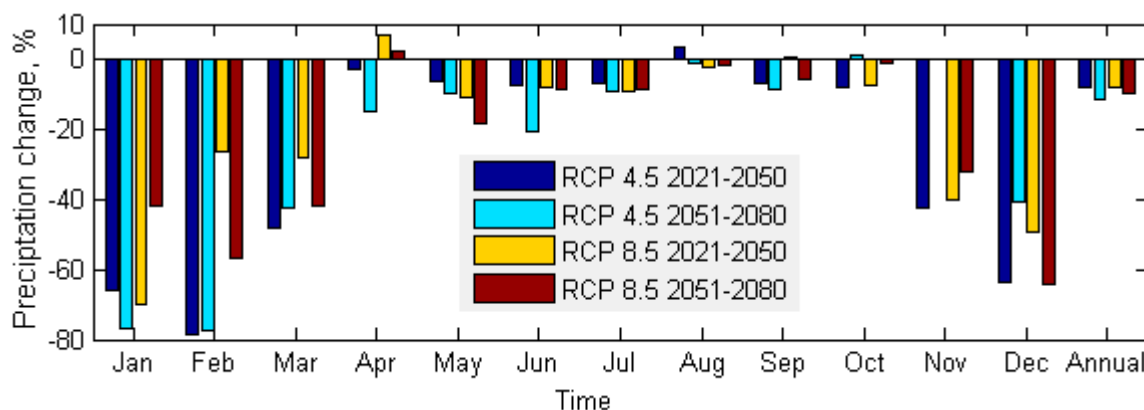
The individual and ensemble mean of the four RCMs were used to assess climate change in two future scenarios; near future (2021–2050) and mid future (2051–2080) with respect to the baseline period (1986–2015) under RCP4.5 and RCP8.5. The results of the projected precipitation by the individual RCMs show a different degree of precipitation changes. Except for HIRHAM5 in mid-term, all the RCMs show precipitation decline under both scenarios. According to CCLM4-8, precipitation decreases by -12.67% under RCP4.5 in near future and -27.47% under RCP8.5 scenarios in a midterm. The highest decline of the precipitation was simulated under RCP8.5 in a mid-term with CCLM4-8 and the lowest decline by HIRHAM5 under RCP4.5 in a midterm. HIRHAM5 shows that precipitation will increase under RCP8.5 scenarios. Summary of RCMs precipitation projections was presented in Table 4.

**Table 4.** Changes in precipitation (%) across the four RCMs in RCP4.5 and RCP8.5 scenarios.

RCMs	RCP4.5		RCP8.5	
	2021–2050	2051–2080	2021–2050	2051–2080
CCLM4-8	−12.67	−15.48	−15.64	−27.47
HIRHAM5	−3.41	−0.89	0.83	4.42
RACMO22T	−9.31	−17.00	−6.39	−4.42
RCA4	−7.57	−11.96	−10.28	−11.22
Ensemble	−8.24	−11.32	−7.87	−9.67

The ensemble mean of the RCMs suggested decreasing precipitation under the two scenarios, like most of the RCMs. The change shows precipitation decline by  $-8.24\%$  under RCP4.5 and  $-7.87\%$  under RCP8.5 in the near-future scenario. Under the mid future, the decline was by  $-11.32\%$  under RCP4.5 and  $-9.67\%$  under RCP8.5. The use of ensemble mean over the individual RCMs helps to minimize the highest and lowest projections and enables to minimize the uncertainties by working with the average of the RCMs. Furthermore, the analysis of the inter-annual and inter-model variability of the climate variables in Finchaa catchment, presented in Dibaba et al. [54], underlines the need to include several climate models in order to cover the range of possible developments.

Changes in projected precipitation are more profound on seasonal bases compared to the annual bases in the catchment. The projected precipitation shows a declining trend in all seasons, except in April by RCP8.5, for both future time horizons and August by RCP4.5 in a near-future scenario. However, the changes are projected higher in the dry season than a wet season as shown by Figure 6. In particular, the seasons with smaller rainfall (March–April–May) are expected to face high precipitation changes while seasons with high rainfall (June–July–August–September) are expected to face lower precipitation change. For dry seasons, all projections give a higher decreasing signal.

**Figure 6.** Percentage change of projected average precipitation in Finchaa catchment for 2021–2050 and 2051–2080 under RCP4.5 and RCP8.5.

In Ethiopia, a decreasing trend of precipitation intensity was reported in eastern, southwestern and southern regions using data ranges from 1965 to 2002 [68]. However, different studies in the Blue Nile basin reported varying changes of precipitation in the future horizon. Elshamy et al. [41] show 10 GCMs out of 17 GCMs reported a reduction of precipitation while the ensemble of the 17 GCMs reports almost no expected precipitation change. On the other hand, Beyene et al. [36] reported an increase in projected precipitation in the late 21st century using 11 GCMs. Large uncertainties among the RCMs-GCMs, regarding the signal of future precipitation, have also been reported in a tropical catchment in a Burkina Faso by de Hipt et al. [69]. The complexity in the nature of precipitation and its dependency on topographic and physical factors could contribute to this.

The results of precipitation projections in this study are consistent with the results presented by climate change studies [16,40]. The study by Daba and Rao [48] on climate change impacts on the

hydro-meteorological variables of Finchaa sub-basin using HadCM GCM also reported decreasing precipitation over the study area. Similarly, the study by Girma [70], using CCLM downscaling for the periods 2041–2070 and 2071–2100, have shown declining precipitation by 6.6% and 6.4% over the upper Blue Nile basin.

### 3.3.2. Temperature

The variation of projected future maximum and minimum temperature is presented in Table 5 for the individual RCMs and their ensemble mean. The result shows that maximum and minimum temperatures increase under both RCPs throughout the study years considered showing the warming trends in the catchment. However, the magnitude of changes by individual RCMs and their mean ensemble is higher for higher emission scenarios (RCP8.5) compared to RCP4.5. Likewise, the change in temperature is higher in the mid future than the near future, under both emission scenarios. Furthermore, there are variations among all the RCMs and the ensemble mean for the degree of the temperature changes. RCA4 have shown the highest increase in maximum temperature under both RCPs during the nearby and mid future.

**Table 5.** Changes in temperature (°C) across the four RCMs in RCP4.5 and RCP8.5 scenarios.

RCMs	RCP4.5		RCP8.5	
	2021–2050	2051–2080	2021–2050	2051–2080
CCLM4-8	1.26	2.01	1.54	3.19
HIRHAM5	1.19	2.07	1.31	3.20
RACMO22T	1.43	2.20	1.42	3.00
RCA4	1.49	2.30	1.71	3.47
Ensemble	1.34	2.15	1.49	3.21

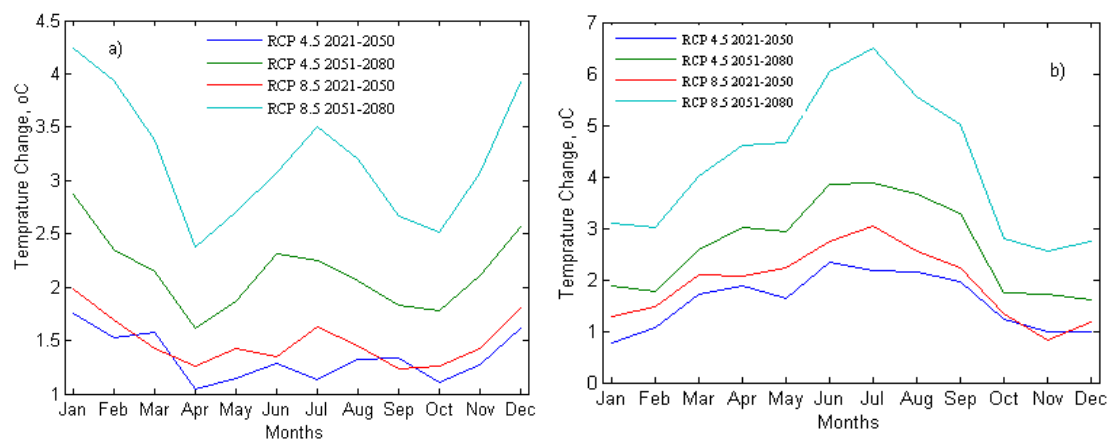
  

RCMs	RCP4.5		RCP8.5	
	2021–2050	2051–2080	2021–2050	2051–2080
CCLM4-8	1.85	3.18	2.32	5.08
HIRHAM5	1.61	2.78	1.76	4.31
RACMO22T	1.45	2.46	1.81	3.92
RCA4	1.39	2.25	1.80	3.60
Ensemble	1.57	2.67	1.92	4.23

Regarding the ensemble mean of the RCMs, the maximum temperature will increase on average by 1.34 °C and 2.15 °C under medium emission scenario (RCP4.5) and minimum temperature increases by 1.57 °C and 2.67 °C for the nearby and mid future, respectively. Likewise, the maximum temperature will increase by 1.49 °C and 3.21 °C and minimum temperature increases by 1.92 °C and 4.22 °C for the near future and mid future respectively under high emission scenarios RCP8.5. Overall, the study revealed the projection of RCP8.5 is warmer than RCP4.5. The highest temperature change in RCP8.5 is also confirmed by Shiferaw et al. [39] using five different GCMs in Ilala watershed, Northern Ethiopia.

The changes in projected temperature were not only expected to vary annually, but they also vary in all seasons. However, the seasonal variations are higher for the minimum temperature than the maximum temperature, as shown in Figure 7. The seasonal changes of maximum temperature is higher in dry seasons (December, January and February), while the rise in minimum temperature is higher in the wet season (June, July, and August). The highest seasonal rise of maximum temperature is reported by RCP8.5 during 2051–2080 while RCP 4.5 reported the lowest rise during 2021–2050.

Like the annual changes, the highest seasonal rise in temperature is expected by the high emission scenario than the medium emission scenario. Likewise, the highest rise in maximum and minimum temperature is expected in the midterm scenario (2051–2080) than the near future (2021–2050).



**Figure 7.** Seasonal projected change in mean maximum temperature (a) and minimum temperature (b) in Finchaa catchment for 2021–2050 and 2051–2080 under RCP4.5 and RCP8.5.

In general, the projection of maximum temperature and minimum temperature in both future time horizons is within the range projected by IPCC and agrees with a range produced by other researchers. Many climate change studies in Ethiopia, in different regions, have shown the temperature is expected to increase. However, the strength of change varies with the techniques of downscaling and climate model types. The study reports by GFDL [71] on climate risk and adaptation country profile, shows mean annual temperature is projected to increase by 1.1 °C to 3.1 °C by the 2060s and 1.5 °C to 5.1 °C by 2090s. The study by Girma [70] also showed the average annual temperature will increase by 1.5 °C, 2.6 °C and 4.5 °C for the periods 2011–2040, 2041–2070 and 2071–2100 respectively over the whole upper Blue Nile basin. The study on the whole Nile Basin by Beyene et al. [36] using the average of 11 GCMs further reported the annual average temperature change of 0.91 °C to 1.9 °C during 2010–2039 for B1 global emission scenarios with respect to 1950–1999 historical periods. Further, the study by Elshamy et al. [41] using 17 GCMs on the Blue Nile projected temperature to increase between 2 °C and 5 °C.

### 3.4. Watershed Hydrological Responses to Land Use/Land Cover and Climate Change

#### 3.4.1. Impacts of Land Use/Land Cover Change

The hydrological responses of the catchment to LULCC was investigated with two LULCC scenarios; first scenario for LULCC of 2017 to 2036 and second scenario for LULCC of 2017 to 2055 with the base land use map of 2017. The hydrological responses of the watershed were considered in terms of the process contributes to the annual surface runoff, annual groundwater, total water yield and potential evapotranspiration as shown in Table 6. Owing to the massive expected changes in land use from 2017 to 2036 and 2017 to 2055, mean annual surface water runoff and total water yield will increase whereas groundwater recharge and potential evapotranspiration will decrease. However, the rate of increase and decline was related to the rate of LULCCs. For example, the rate of agricultural expansion and forest decline was predicted to be higher in the first scenario and lower in the second. Consequently, the rate of increase in surface flow was lower, increasing from 2036 to 2055, compared to the baseline scenario. In general, the impacts of the LULCC are related to the increase of agricultural lands coupled with the decrease of forestlands.

**Table 6.** Variation of the annual water balance components under LULCC.

Land Use	Surface Runoff (%)	Groundwater (%)	Water Yield (%)	PET (%)
2036	5.97	−1.09	1.94	−1.15
2055	7.11	−0.92	2.26	−1.36

The increase in surface runoff and water yield is 5.97% and 1.9% in the first scenario and 7.1% and 2.26% in the second scenario, respectively. The groundwater and potential evapotranspiration declines by 1.09% and 1.15% in the first and 0.91%, and 1.36% in the second scenario, respectively. As it can be seen from Figure 8, the decline of groundwater in the second scenario was lower than the first scenario owing to the increase of the predicted shrublands in 2055, compared to 2036 LULC. Hence, the decreasing rate is higher for the changes in 2017 to 2036, where the rate of forest and shrubland decline is higher. This is a good indication to see the effect of works with changing the land cover in groundwater management i.e., if shrubland increases, then groundwater recharge will increase. The decrease in evapotranspiration was due to the decline of evapotranspiration owing to the decline of forestland. Further, the decline in evapotranspiration could also be related to the shortage of soil moisture as a result of increased runoff. A similar study showed that PET decreases with the shortage of soil moisture as a result of reduced rainfall [72].

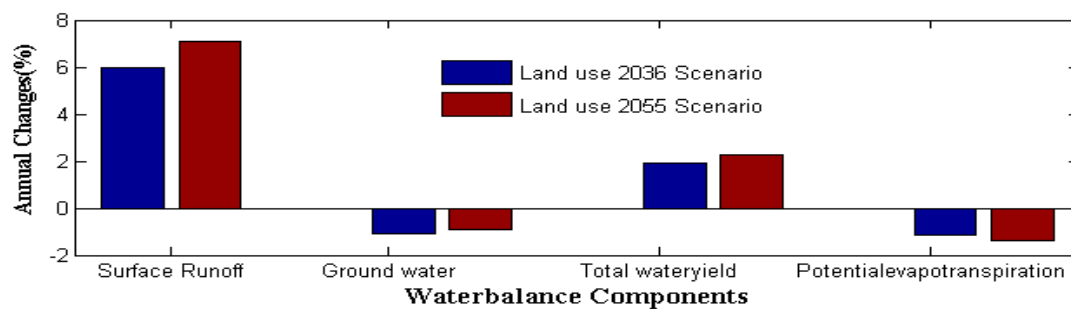
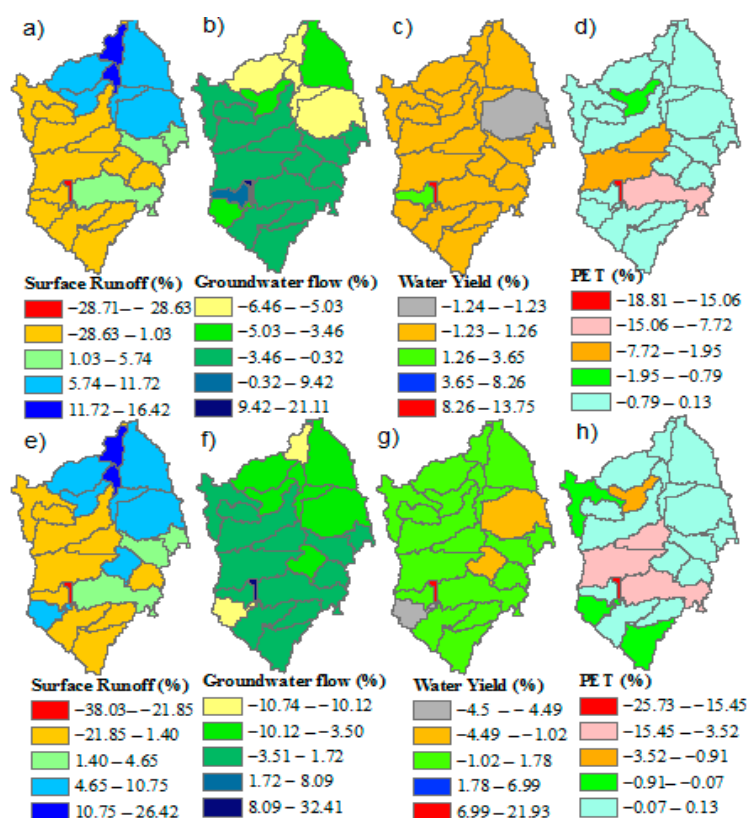


Figure 8. Impacts of land use/ land cover change on water balance.

The spatial distribution of the hydrological process under the projected LULCC for 2017–2036 is presented by Figure 9a–d and for 2017–2055 presented by Figure 9e–h. Each sub-basin has different characteristics of a hydrological process. The highest increase in surface runoff is around the downstream while the upstream area shows a decline of the surface runoff under both scenarios with the highest increase and decrease expected in the second scenario. Areas with a high decline of surface runoff show an increase in groundwater. This demonstrates that surface runoff is inversely correlated with groundwater under both scenarios. The high decline in PET is expected around the central parts of the catchment, while the upstream areas are characterized by low decline. Water yield shows high decline around the northeast part in the first scenario and southwestern part in the second scenario. However, the majority of the sub-basins show an increase in water yield with the highest increase shown by the second scenario.

The highest increase in surface flow and decline of groundwater recharge is associated with the highest expansion of agricultural lands and urban expansion and decline of forest and shrubland. This reveals a massive conversion of LULC to intensive agriculture and settlements will reduce the soil infiltrations capacity, causing a large portion of rainfall directly changed to surface runoff. The reduction of soil water infiltration, in turn, causes groundwater flow decline. Furthermore, the increasing demand for the growing population to use groundwater could additionally contribute to the decline of groundwater by increasing groundwater withdrawal. The recent evidence by Dibaba et al. [2] in Finchaa catchment reported that, due to the high changes in LULC, springs in the catchment are dried out, and the level of water in hand-bug wells decline. Further, the finding agrees with the study by Shi et al. [73] who indicated the main effects of LULCC on the water cycle are changes in evapotranspiration (ET), the soil's ability to hold water and in the abilities of vegetation to intercept precipitation.



**Figure 9.** Spatial patterns of the changes in surface runoff, groundwater, water yield and PET due to LULCC. The top panel (a–d) shows the first scenario (2017–2036) and the bottom (e–h) shows the second scenario (2017–2055).

The increase in surface water has increased the total water yield of the catchment. This indicates that degraded watersheds can accelerate surface runoff by reducing both the retention as soil water and groundwater recharge. Consequently, the catchment will face severe soil erosion, landslides and flash floods. This could become a great concern where mega hydropower projects exist. Overall, surface runoff, water yield and potential evapotranspiration were found to be more sensitive than the groundwater flow in Finchaa catchment under LULCC.

The findings of the study are consistent with various research studies conducted in other catchments. For instance, Gashaw et al. [74] in Andessa catchment, Ethiopia concluded that the changes in land use have reduced groundwater flow and increased surface runoff. Shawul et al. [18] also showed an increased surface runoff and decline of groundwater between 1974–2014 in upper Awash basin was attributed by the LULCCs of the catchment. However, the study reported that the magnitude of the groundwater fluctuation is much less compared to the surface runoff. A previous study in the Finchaa catchment, in LULCC from 1987 to 2017, shows that construction of Fincha, Neshe and Amerti hydropower projects along with irrigation projects have brought a dramatic LULCC [2]. Consequently, the scarcity of land coupled with the need to farm more lands has led the community to cultivate steep slopes. The cultivation of steep slopes, in turn, increased the vulnerability of land to soil erosion, which reduced the water resources of the catchment.

### 3.4.2. Impacts of Climate Change

Changes in rainfall and temperature were used to predict the impacts of climate change on water balance components of the catchment. Consequently, the projected changes in mean annual precipitation and temperature, under the two RCPs, caused a significant variation in the projected water balance components of Finchaa catchment.

SWAT simulations for the near future and mid future showed that the decline of precipitation and increase of temperature will lead to reduced surface flow, groundwater and overall water yield (Table 7). Changes in temperature and PET are correlated positively. Consequently, the increase in temperature resulted in increased potential evapotranspiration and evaporation, which could be a critical factor for the decline of water yield. As the forms of water are subjected to losses, owing to the changes in temperature, evaporation is also a factor for the future decline of the surface runoff. This is expected considering the warming trends of temperature.

**Table 7.** Changes of water balance components under a climate change.

Scenario	Period	Surface Runoff (%)	Groundwater (%)	Water Yield (%)	PET (%)
RCP4.5	2021–2050	−7.334	−9.21	−8.49	16.31
	2051–2080	−14.48	−13.7	−13.77	19.24
RCP8.5	2021–2050	−12.32	−9.56	−10.32	16.9
	2051–2080	−9.3	−15.86	−13.51	22.89

In general, the impacts of the climate changes on the watershed hydrology can be explained with the combinations of precipitation, temperature and evapotranspiration. Decreased rainfall reduces surface runoff and increasing temperatures amplified the increase in evapotranspiration, which may have resulted in the decreased runoff. In this regard, the correlation between precipitation and the simulated surface runoff, groundwater and total water yield is positive, while the relationship between the temperature and hydrological process are positive only for PET. However, the relationship between the precipitation and temperature with the hydrological process varies with the RCPs and period of the scenario. For example, changes in precipitation and the predicted decline of groundwater and total water yields are higher during 2051–2080 under both RCPs. However, the decline of surface runoff is only higher under RCP4.5 during the 2051–2080 (14.48%). Under RCP8.5, surface water decline is higher during 2021–2050 (−12.32%) as shown in Figure 10. This shows that change in precipitation alone is not the only variable that affects surface water. This finding was consistent with other research reports in the Nile River [41,75]. According to Coffel et al. [75], dry and hot years driven by increasing regional temperatures are becoming more frequent in the upper Nile.

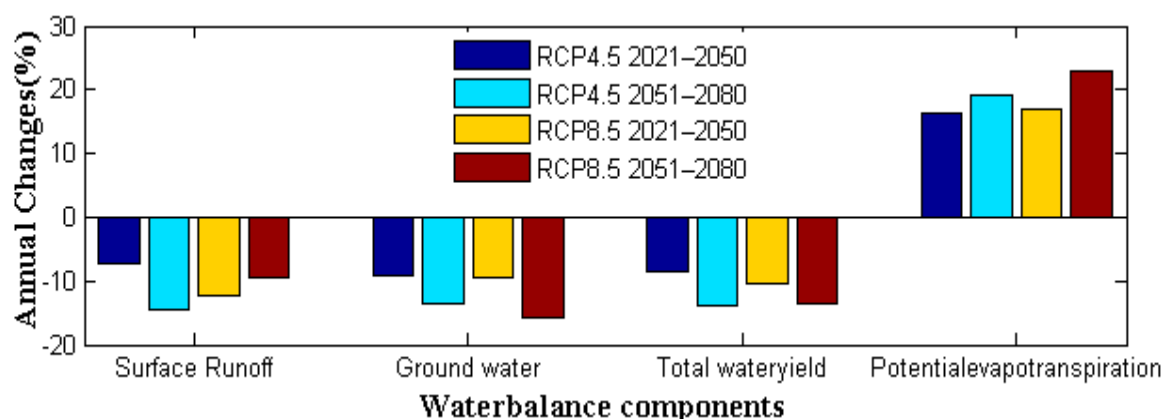


**Figure 10.** Impacts of climate change on water balance.

The spatial distribution of the hydrological process under the projected climate change for RCP4.5 and RCP8.5 is presented in Figure 11a–d for surface runoff, Figure 11e–h for groundwater, Figure 11i–l for water yield and Figure 11m–p for PET. Although the impacts of climate change reported a reduction of surface runoff, groundwater and water yield in the catchment, each sub-basin is characterized by different yields. The changing spatiotemporal patterns and magnitudes of precipitation are expected to directly disturb the hydrological process, while indirect impacts are expected from changes in temperature. Commonly, the highest decline of the surface runoff, groundwater, and water yield is

projected around the upstream of the catchment, under both scenarios throughout the study projections considered. The projection of surface runoff and water yield decline is higher under RCP4.5 and RCP8.5 scenarios in the mid future than the near future. The lowest decline of surface runoff under both scenario is projected around the southwestern part in the near future and northeastern in the mid future. Groundwater and water yield decline is higher around the southwestern part. The highest rise in PET is shown by RCP8.5 around the outlet of the catchment in the mid future projection.

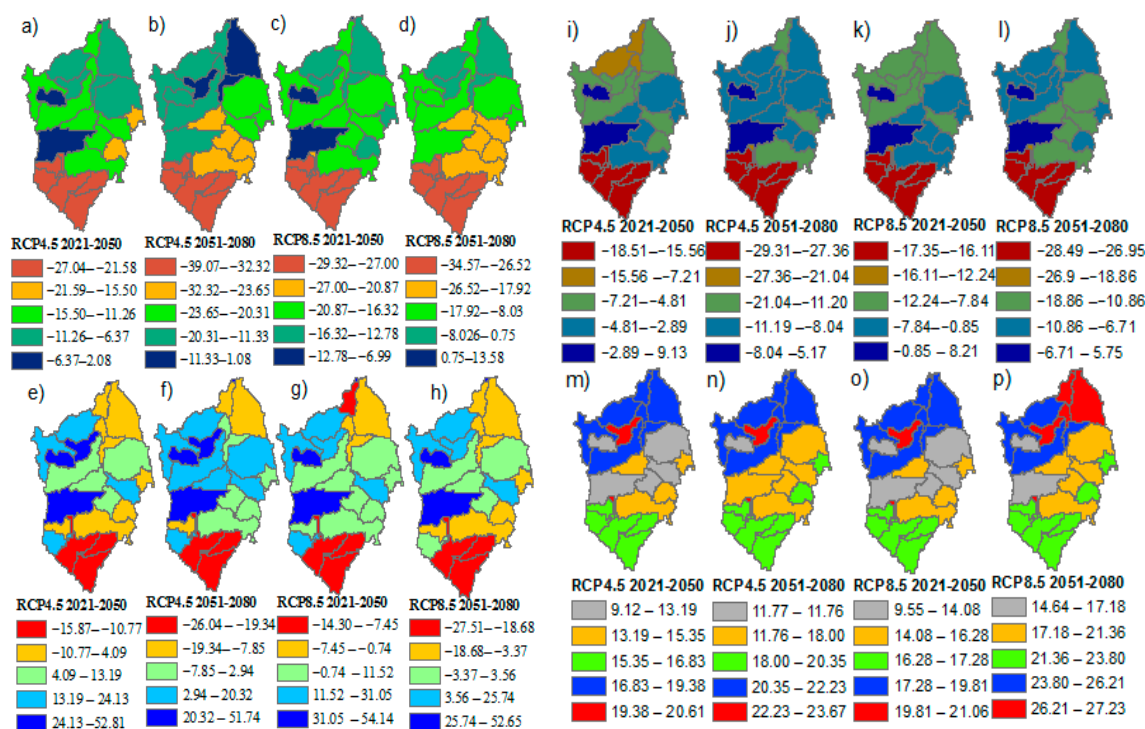


**Figure 11.** Spatial patterns of the changes in surface runoff (a–d), groundwater (e–h), water yield (i–l) and PET (m–p) due to CC.

Generally, the decrease in average annual flow over the catchment could be due to the annual and seasonal decrease of precipitation and increase in temperature under both scenarios. The possibility of surface water, groundwater and total water yield reduction in the catchment could affect the availability of water resources in the catchment and further aggravate water stress in the downstream. The acceleration of the increasing water abstractions could also contribute to the further decline in water resources besides the climate change pressure.

The increase in PET due to high-temperature increase coupled with decreasing precipitation could also lead to reduced soil moisture, which is required for plant growth and groundwater storage. This could imply the reduced availability of water for crop production, which will become chronic to the farmers in the catchment whose livelihood is based on agriculture alone. Further, an increase in temperature led to increased PET, this in turn, resulted in an increased need for irrigation.

Climate change studies on Africa, sub-Saharan, in particular, confirmed similar findings as climate projections show a range of warming trends in inland subtropics, a frequent occurrence of extreme heat events, increasing aridity and changes in rainfall [76]. According to Serdeczny et al. [76] the impacts due to climate change add significant impact on the existing undernutrition, infectious disease, the vulnerability of rain-fed agriculture and flash flooding crises in the region.

The finding also confirms the findings of Beyene et al. [36] which showed the Nile river is expected to decline during the mid. 2040–2069 and late 2070–2099 due to the decline in precipitation and increased evaporation demand. The study by Gebremeskel and Kebede [77] on climate change impacts on water sources of the Tekeze river basin also predicted the decline of surface runoff by 13% and 14%.

The study by Shiferaw et al. [39] using the ensemble of five GCMs also confirmed the decline of the projected surface runoff under both RCPs due to climate change.

### 3.4.3. Impacts of Land Use/Land Cover and Climate Change

Although the direct effect of a decline in precipitation and increased temperature disturbs the hydrology of the catchment as presented under the impacts of climate change, changes in LULC with soil and vegetation properties, either enhance or decrease the impacts of climate change. In this regard, the effects of combined LULC and climate change on the hydrological process was done to distinguish the effects of LULC and climate change under the isolated and combined scenarios.

The increase of temperature and decreasing precipitation under a varying LULC in Finchaa catchment shows a decline of surface runoff, groundwater and total water yield, whereas the projected evapotranspiration is increasing. The combined effects of LULC and climate change on the watershed hydrological process are presented in Table 8. The highest annual surface runoff decline of 9.09% is projected under the RCP4.5 in a midterm scenario, and the highest groundwater decline of 15.30% is projected under RCP8.5 in the midterm period.

**Table 8.** Changes of water balance components under a combined land use/land cover and climate change.

Scenario	Period	Surface Runoff (%)	Groundwater (%)	Water Yield (%)	PET (%)
RCP4.5	2021–2050	−1.79	−8.65	−6.31	14.86
	2051–2080	−9.09	−13.11	−11.63	17.50
RCP8.5	2021–2050	−6.97	−8.95	−8.17	15.44
	2051–2080	−3.87	−15.30	−11.37	21.13

As presented in Figure 12, both RCPs projected a higher decline of the water yield and groundwater during the mid-future scenario. Similarly, the highest increase in PET is projected during the mid-future for both RCPs.

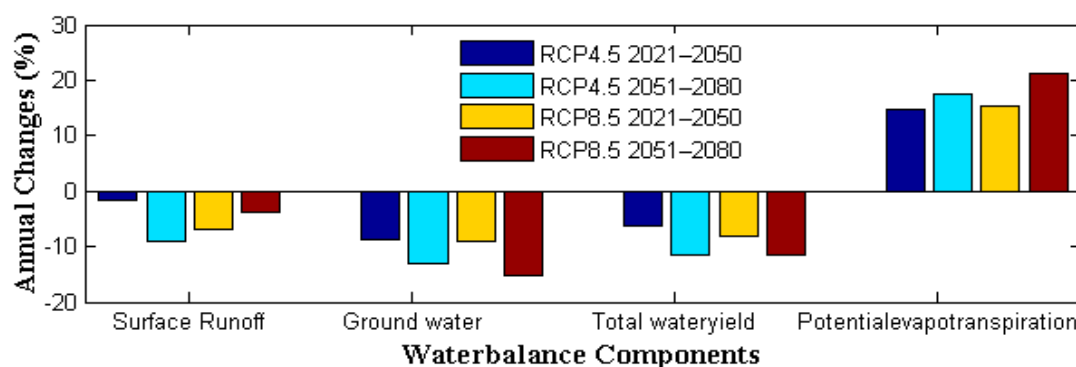


**Figure 12.** Annual water balance components under the combined land use and climate change.

The spatial distribution of the hydrological process under the projected LULC and climate change under the RCP4.5 and RCP8.5 are presented in Figure 13a–d for surface runoff, Figure 13e–h for groundwater, Figure 13i–l for water yield and Figure 13m–p for PET. The reduction in surface runoff is lower around the downstream of the catchment under all scenarios, while the high decline is around upstream of the catchment. Higher groundwater decline is expected around the upstream and outlet of the catchment, with the highest decline under RCP8.5 in the late scenario. Water yield is projected to decline higher around the upstream while a high increase in PET is projected around the downstream of the catchment.

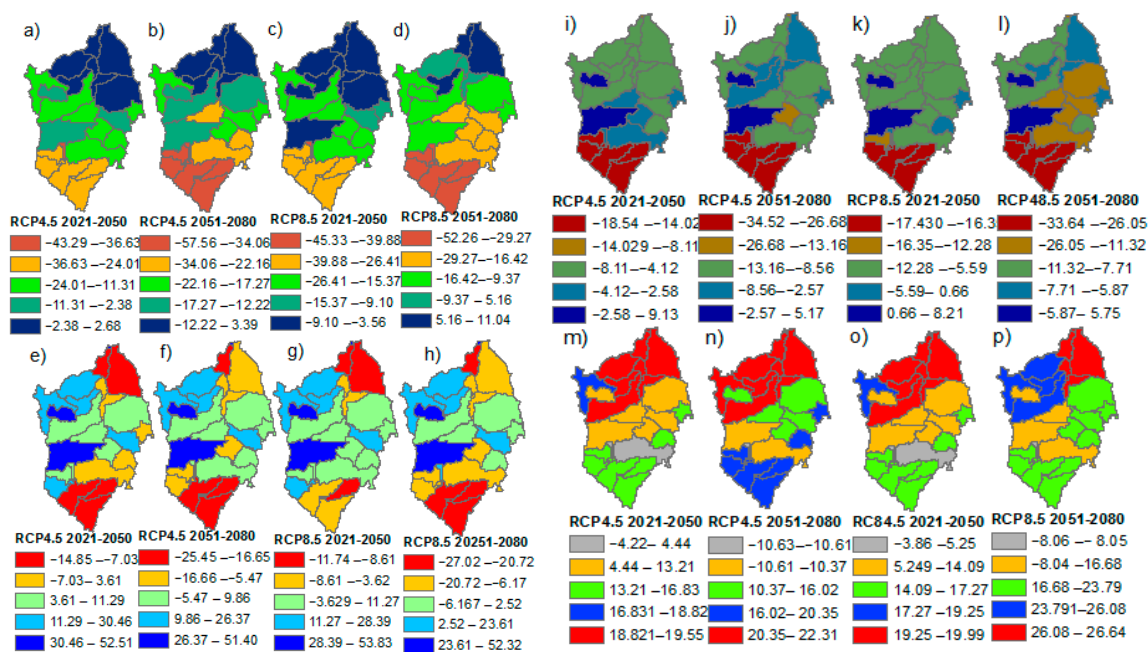


**Figure 13.** Spatial patterns of the changes in surface runoff (a–d), groundwater (e–h), water yield (i–l) and PET (m–p) under the combined LULCC and climate change.

The increasing temperature is the most dominant factor affecting surface runoff in climate change scenarios while increasing urbanization is the main contributor affecting the surface runoff in LULC scenarios. Overall, the increase in surface runoff and total water yield due to LULCC was offset by the decline of the surface runoff and total water yield, due to climate change impacts. Consequently, the effect of climate change is decisive compared to the LULCC in the Finchaa catchment. The high sensitivity of water balance components and streamflow to the climate change is also reported by other studies in different parts of the world [22,72,73,78,79]. For example, the study by Shi et al. [73] in the upstream of Huai River, China reported that the combined effect of LULC and climate change has increased surface water, evapotranspiration and streamflow. However, the differentiated impacts of LULC and climatic variability on hydrological process shows a change in streamflow because of the effects of climate variability on the hydrological process were offset by the effect of LULCC. A combined study of LULC and climate change in Hoeya River Basin of Korea by Kim et al. [79] also shows that the combined scenario was similar to that of climate change only scenario.

In summary, the seasonal and annual variation of the future temperature shows the increased hot and dry years that will lead to serious water scarcity. Consequently, the increase in warming and evaporation in the catchment highly affects the three reservoirs in the catchment increasing water stress. The recent study by Coffel et al. [75] also revealed that the increase in regional temperature indicates the water balance of the Blue Nile basin may become moisture constrained in the future. The study report also shows the trend continues despite the increasing precipitation projected by climate models. The decline of the runoff amplifies the effects of water security in the catchment. With the LULC and climate changes, the soil moisture required for crop growth is reduced, and land degradation problems of the Finchaa catchment, occur as the landslide and gully become severe. The research studies by Vlek et al. [13] further reported that land degradations are related to the deterioration in climate conditions and human intervention.

Although the study did not cover the quantification of sediment yield, the SWAT simulation, under the LULCC, shows that the sediment yield increases with the changes. However, sediment yield is decreasing with the projected scenarios of climate change. The study by Gadissa et al. [40] on the effects of climate change on sedimentation in the Rift valley basin of Ethiopia reported a decrease of sediment yield by 38% under RCP4.5 and by 23% under RCP8.5. Therefore, the study further suggests

the need to study the impacts of the combined LULC and climate change on the sedimentation in Finchaa catchment for better sediment management.

#### 4. Conclusions

Four RCMs and their ensemble mean, under CORDEX-Africa, were applied for the climate change study. The simulations of all RCMs, except HIRHAM5, show decreasing precipitation under both high and medium-low emission scenarios. With respect to temperature, all RCMs projections show an increasing temperature with varying degree of changes. To avoid the considerable variations of the individual RCMs in projecting precipitation and temperature, the ensemble mean of the RCMs were used for the hydrological impact studies of climate changes, and the combined LULC and climate change. Although uncertainties of climate prediction still exist, the use of the ensemble RCMs was found to be a suited strategy to evaluate the uncertainties of individual RCMs.

The findings from this work were applied to distinguish the effects of LULC and climate change on the water balance components of the Finchaa catchment. Consequently, the metro-hydrological process could change in probability and intensity due to climate change, but also due to local land use/land cover change. If climate change is considered alone, the increase in temperature and decrease of predicted precipitation will decrease the surface runoff, groundwater and total water yield, whereas potential evapotranspiration and evaporation increase. However, the surface runoff increases under land use/land cover changes, due to the highly expanding urbanization and intensive agriculture. Overall, the sensitivity of water resources for land use/land cover and climate change over Finchaa catchment shows the effect of land use/land cover change is stunned by the effects of climate change. Consequently, climate change is found to be predominant over the effects of LULCC.

Further, the seasonal and annual variation of the future precipitation and temperature in the catchment shows the increasingly hot and dry years that will lead to serious water scarcity. Consequently, the catchment is highly vulnerable to climate change and its impacts could range from warming to crop failures as a result of prolonged dry seasons. The Upper Blue Nile basin will face regional water scarcity regardless of whether the precipitation is increased, constant or decreased [75]. The decline of the runoff amplifies the effects of water security in the catchment.

The study analysis suggests that the impact assessments of the combined land use/land cover and climate change in the Finchaa catchments are well-represented by the SWAT simulations. However, the limited availability and quality of hydro-climatic data in the region need urgent attention to improve our understanding of the change in existing and future climate and LULCCs.

The findings of this study provided important information on the relative influences of how the watershed hydrological process in Finchaa catchment respond to the changes in land use/land cover and climate change. This could help to plan proper water resources management interventions. If the degraded sloppy lands are rehabilitated, the ground recharge increase and the surface runoff, which washes the topsoil into the lakes, is reduced. Furthermore, the three lakes in the catchment should be buffered with proper management strategies. In general, the result highlights the need for regional developments and cooperation to urge strong climate-resilient management strategies and to counteract the rapid climate changes in the catchment.

**Author Contributions:** Conceptualization, W.T.D. and T.A.D.; methodology, W.T.D.; software, W.T.D.; validation, W.T.D., T.A.D. and K.M.; formal analysis, W.T.D.; investigation, W.T.D.; resources, T.A.D.; writing—original draft preparation, W.T.D.; writing—review and editing, T.A.D. and K.M.; supervision, T.A.D. and K.M. All authors have read and agreed to the published version of the manuscript.

**Funding:** This research received no external funding.

**Acknowledgments:** We would like to thank Rostock University, Jimma University, and the Centre of Excellence in Science and Technology, Ethiopia, for providing resources and material supports for the study. The RCMs data are obtained from the <https://climate4impact.eu/impactportal/data/esgfsearch.jsp>. We thank the world climate Research Program (WCRP), IS-ENES Climate4Impact for providing the data sets of the Coordinated Regional Downscaling Experiment (CORDEX). We also thank the National Meteorological Agency for providing observed climate data. It is our pleasure to thank Wakene Negassa, who helped us with English language editing.

**Conflicts of Interest:** The authors declare no conflict of interest.

## References

1. Oliver, T.H.; Morecroft, M.D. Interactions between climate change and land use change on biodiversity: Attribution problems, risks, and opportunities. *Wiley Interdiscip. Rev. Clim. Chang.* **2014**, *5*, 317–335. [[CrossRef](#)]
2. Dibaba, W.T.; Demissie, T.A.; Miegel, K. Drivers and implications of land use/land cover dynamics in finchaa catchment, Northwestern Ethiopia. *Land* **2020**, *9*, 113. [[CrossRef](#)]
3. Githui, F.; Mutua, F.; Bauwens, W. Estimating the impacts of land-cover change on runoff using the soil and water assessment tool (SWAT): Case study of Nzoia catchment, Kenya/Estimation des impacts du changement d’occupation du sol sur l’écoulement à l’aide de SWAT: Étude du cas du bassin. *Hydrol. Sci. J.* **2009**, *54*, 899–908. [[CrossRef](#)]
4. Msofe, N.K.; Sheng, L.; Lyimo, J. Land use change trends and their driving forces in the kilombero valley floodplain, Southeastern Tanzania. *Sustainability* **2019**, *11*, 505. [[CrossRef](#)]
5. Hill, J.; Stellmes, M.; Udelhoven, T.; Röder, A.; Sommer, S. Mediterranean desertification and land degradation Mapping related land use change syndromes based on satellite observations. *Glob. Planet. Chang.* **2008**, *64*, 146–157. [[CrossRef](#)]
6. Greco, M.; Mirauda, D.; Squicciarino, G.; Telesca, V. Advances in Geosciences Desertification risk assessment in southern Mediterranean areas. *Adv. Geosci.* **2005**, *2*, 243–247. [[CrossRef](#)]
7. Luck, M.; Landis, M.; Gassert, F. *Aqueduct Water Stress Projections: Decadal Projectons of Water Supply and Demand Using CMP5 GCMs*; Technical Note; World Resources Institute: Washington, DC, USA, 2015; pp. 1–20. Available online: <https://www.wri.org/publication/aqueduct-water-stress-projections> (accessed on 26 March 2020).
8. Getachew, H.E.; Melesse, A.M. The Impact of Land Use Change on the Hydrology of the Angereb Watershed, Ethiopia. *Int. J. Water Sci.* **2012**, *1*, 4. [[CrossRef](#)]
9. Lambin, E.F.; Turner, B.L.; Geist, H.J.; Agbola, S.B.; Angelsen, A.; Bruce, J.W.; Coomes, O.T.; Dirzo, R.; Fischer, G.; Folke, C.; et al. The causes of land-use and land-cover change: Moving beyond the myths. *Glob. Environ. Chang.* **2001**, *11*, 261–269. [[CrossRef](#)]
10. Foley, J.A.; DeFries, R.; Asner, G.P.; Barford, C.; Bonan, G.; Carpenter, S.R.; Chapin, F.S.; Coe, M.T.; Daily, G.C.; Gibbs, H.K.; et al. Global consequences of land use. *Science* **2005**, *309*, 570–574. [[CrossRef](#)]
11. Legesse, D.; Vallet-Coulomb, C.; Gasse, F. Hydrological response of a catchment to climate and land use changes in Tropical Africa: Case study south central Ethiopia. *J. Hydrol.* **2003**, *275*, 67–85. [[CrossRef](#)]
12. Tomer, M.D.; Schilling, K.E. A simple approach to distinguish land-use and climate-change effects on watershed hydrology. *J. Hydrol.* **2009**, *376*, 24–33. [[CrossRef](#)]
13. Vlek, P.; Tamene, L.; Martius, C.; Lamers, J.; Drechsel, P.; Ziadat, F.M.; Le, Q.B.; Mirzabaev, A.; Nkonya, E.; Lynden, G.V.; et al. *Land Degradation and the Sustainable Development Goals: Threats and Potential Remedies*; CIAT Publication No. 440; International Center for Tropical Agriculture (CIAT): Nairobi, Kenya, 2017.
14. Guo, H.; Hu, Q.; Jiang, T. Annual and seasonal streamflow responses to climate and land-cover changes in the Poyang Lake basin, China. *J. Hydrol.* **2008**, *355*, 106–122. [[CrossRef](#)]
15. Tu, J. Combined impact of climate and land use changes on streamflow and water quality in eastern Massachusetts, USA. *J. Hydrol.* **2009**, *379*, 268–283. [[CrossRef](#)]
16. Dile, Y.T.; Berndtsson, R.; Setegn, S.G. Hydrological Response to Climate Change for Gilgel Abay River, in the Lake Tana Basin—Upper Blue Nile Basin of Ethiopia. *PLoS ONE* **2013**, *8*, e79296. [[CrossRef](#)] [[PubMed](#)]
17. Takala, W.; Adugna, T.; Tamam, D. The effects of land use land cover change on hydrological process of Gilgel Gibe, Omo Gibe Basin, Ethiopia. *Int. J. Sci. Eng. Res.* **2016**, *7*, 117–128.
18. Shawul, A.A.; Chakma, S.; Melesse, A.M. The response of water balance components to land cover change based on hydrologic modeling and partial least squares regression (PLSR) analysis in the Upper Awash Basin. *J. Hydrol. Reg. Stud.* **2019**, *26*, 1–19. [[CrossRef](#)]
19. Karimi, H.; Jafarnejhad, J.; Khaledi, J.; Ahmadi, P. Monitoring and prediction of land use/land cover changes using CA-Markov model: A case study of Ravansar County in Iran. *Arab. J. Geosci.* **2018**, *11*, 592. [[CrossRef](#)]

20. Yang, C.; Wu, G.; Chen, J.; Li, Q.; Ding, K.; Wang, G. Simulating and forecasting spatio-temporal characteristic of land-use/cover change with numerical model and remote sensing: A case study in Fuxian Lake Basin, China. *Eur. J. Remote Sens.* **2019**, *52*, 374–384. [[CrossRef](#)]
21. Liping, C.; Yujun, S.; Saeed, S. Monitoring and predicting land use and land cover changes using remote sensing and GIS techniques—A case study of a hilly area, China. *PLoS ONE* **2018**, *13*, e200493. [[CrossRef](#)]
22. Pan, S.; Liu, D.; Wang, Z.; Zhao, Q.; Zou, H.; Hou, Y.; Liu, P.; Xiong, L. Runoff Responses to Climate and Land Use/Cover Changes under Future Scenarios. *Water* **2017**, *9*, 475. [[CrossRef](#)]
23. Hamad, R.; Balzter, H.; Kolo, K. Predicting Land Use/Land cover changes using a ca-markov model under two different scenarios. *Sustainability* **2018**, *10*, 3421. [[CrossRef](#)]
24. Qi, S.; Sun, G.; Wang, Y.; McNulty, S.G.; Myers, J.A.M. Streamflow response to climate and landuse changes in a coastal watershed in North Carolina. *Am. Soc. Agric. Biol. Eng.* **2009**, *52*, 739–749.
25. Asner, G.P.; Loarie, S.R.; Heyder, U. Combined effects of climate and land-use change on the future of humid tropical forests. *Conserv. Lett.* **2010**, *3*, 395–403. [[CrossRef](#)]
26. Rahman, K.; da Silva, A.G.; Tejada, E.M.; Gobiet, A.; Beniston, M.; Lehmann, A. An independent and combined effect analysis of land use and climate change in the upper Rhone River watershed, Switzerland. *Appl. Geogr.* **2015**, *63*, 264–272. [[CrossRef](#)]
27. El-Khoury, A.; Seidou, O.; Lapen, D.R.L.; Que, Z.; Mohammadian, M.; Sunohara, M.; Bahram, D. Combined impacts of future climate and land use changes on discharge, nitrogen and phosphorus loads for a Canadian river basin. *J. Environ. Manag.* **2015**, *151*, 76–86. [[CrossRef](#)]
28. Mekonnen, D.F.; Duan, Z.; Rientjes, T.; Disse, M. Analysis of the combined and single effects of LULC and climate change on the streamflow of the Upper Blue Nile River Basin (UBNRB): Using statistical trend tests, remote sensing landcover maps and the SWAT model. *Hydrol. Earth Syst. Sci. Discuss.* **2017**, 1–26. [[CrossRef](#)]
29. Zamora-Gutierrez, V.; Pearson, R.G.; Green, R.E.; Jones, K.E. Forecasting the combined effects of climate and land use change on Mexican bats. *Divers. Distrib.* **2018**, *24*, 363–374. [[CrossRef](#)]
30. Langerwisch, F.; Vaclavik, T.; Von Bloh, W.; Vetter, T.; Thonicke, K. Combined effects of climate and land-use change on the provision of ecosystem services in rice agro-ecosystems. *Environ. Res. Lett.* **2018**, *13*, 1. [[CrossRef](#)]
31. Combalicer, E.A.; Im, S. Change Anomalies of Hydrologic Responses to Climate Variability and Land-use Changes in the Mt. Makiling Forest Reserve. *J. Environ. Sci. Manag.* **2012**, *1*, 1–13.
32. Yalew, S.G.; Mul, M.L.; van Griensven, A.; Teferi, E.; Priess, J.; Schweitzer, C.; Zaag, P. van Der. Land-use change modelling in the Upper Blue Nile Basin. *Environments* **2016**, *3*, 21. [[CrossRef](#)]
33. Gashaw, T.; Tulu, T.; Argaw, M.; Worqlul, A.W. Evaluation and prediction of land use/land cover changes in the Andassa watershed, Blue Nile Basin, Ethiopia. *Environ. Syst. Res.* **2017**, *6*, 1–15. [[CrossRef](#)]
34. Gidey, E.; Dikinya, O.; Sebego, R.; Segosebe, E.; Zenebe, A. Cellular automata and Markov Chain (CA\_Markov) model-based predictions of future land use and land cover scenarios (2015–2033) in Raya, Northern Ethiopia. *Model. Earth Syst. Environ.* **2017**, *3*, 1245–1262. [[CrossRef](#)]
35. Hishe, S.; Bewket, W.; Nyssen, J.; Lyimo, J. Analyzing past land use land cover change and CAMarkov based future modeling in the Middle Suluh Valley, Northern Ethiopia. *Geocarto Int.* **2018**. [[CrossRef](#)]
36. Beyene, T.; Lettenmaier, D.P.; Kabat, P. Hydrologic impacts of climate change on the Nile River Basin: Implications of the 2007 IPCC scenarios. *Clim. Chang.* **2010**, *100*, 433–461. [[CrossRef](#)]
37. Ashenafi, A.A. Modeling Hydrological Responses to Changes in Land Cover and Climate in Geba River Basin, Northern Ethiopia. Ph.D. Thesis, Freie Universität, Berlin, Germany, 2014.
38. Gebre, S.L.; Ludwig, F. Hydrological response to climate change of the Upper Blue Nile River Basin: Based on IPCC fifth assessment report (AR5). *J. Climatol. Weather Forecast.* **2015**, *3*, 1–15. [[CrossRef](#)]
39. Shiferaw, H.; Gebremedhin, A.; Gebretsadkan, T.; Zenebe, A. Modelling hydrological response under climate change scenarios using SWAT model: The case of Ilala watershed, Northern Ethiopia. *Model. Earth Syst. Environ.* **2018**, *4*, 437–449. [[CrossRef](#)]
40. Gadissa, T.; Nyadawa, M.; Behulu, F.; Mutua, B. The effect of climate change on loss of lake volume: Case of sedimentation in Central Rift Valley. *Hydrology* **2018**, *5*, 67. [[CrossRef](#)]
41. Elshamy, M.E.; Seierstad, I.A.; Sorteberg, A. Impacts of climate change on Blue Nile flows using bias-corrected GCM scenarios. *Hydrol. Earth Syst. Sci.* **2009**, *13*, 551–565. [[CrossRef](#)]
42. Liniger, H.; Mekdaschi Studer, R.; Hauert, C.; Gurtner, M. *Sustainable Land Management in Practice—Guidelines and Best Practices for Sub-Saharan Africa*; TerrAfrica, World Overview of Conservation Approaches and Technologies (WOCAT) and Food and Agriculture Organization of the United Nations (FAO): Rome, Italy, 2011.

43. Taye, M.T.; Willems, P.; Block, P. Implications of climate change on hydrological extremes in the Blue Nile basin: A review. *J. Hydrol. Reg. Stud.* **2015**, *4*, 280–293. [[CrossRef](#)]
44. Ayana, A.B.; Edossa, D.C.; Kositsakulchai, E. Modeling the effects of land use change and management practices on runoff and sediment yields in Fincha watershed, Blue Nile. *OIDA Int. J. Sustain. Dev.* **2014**, *7*, 75–88.
45. Kitila, G.; Gebrekidan, H.; Alamrew, T. Soil Quality Attributes Induced by Land Use Changes in the Fincha'a Watershed, Nile Basin of Western Ethiopia. *Sci. Technol. Arts Res. J.* **2016**, *5*, 16–26. [[CrossRef](#)]
46. Tefera, B.; Sterk, G. Hydropower-Induced Land Use Change in Fincha'a Watershed, Western Ethiopia: Analysis and Impacts. *Mt. Res. Dev.* **2008**, *28*, 72–80. [[CrossRef](#)]
47. Koch, M.; Cherie, N. SWAT-Modeling of the Impact of future Climate Change on the Hydrology and the Water Resources in the Upper Blue Nile River Basin, Ethiopia. In Proceedings of the 6th International Conference on Water Resources and Environment Research, ICWRER, Koblenz, Germany, 3–7 June 2013.
48. Daba, M.; Rao, G.N. Evaluating Potential Impact of Climate Change on Hydro-meteorological Variables in Upper Blue Nile Basin. A Case Study Fincha Sub-Basin. *J. Environ. Earth Sci.* **2016**, *6*, 48–57.
49. Bewket, W.; Sterk, G. Dynamics in land cover and its effect on stream flow in the Chemoga watershed, Blue Nile basin, Ethiopia. *Hydrol. Process.* **2005**, *19*, 445–458. [[CrossRef](#)]
50. Melesse, A.M.; Loukas, A.G.; Senay, G.; Yitayew, M. Climate change, land-cover dynamics and ecohydrology of the Nile River Basin. *Hydrol. Process.* **2009**, *23*, 3651–3652. [[CrossRef](#)]
51. Senbeta, F. Community perception of land use/land cover change and its impacts on biodiversity and ecosystem services in northwestern Ethiopia. *J. Sustain. Dev. Afr.* **2018**, *20*, 108–126.
52. Geleta, C.D.; Gobosho, L. Climate Change Induced Temperature Prediction and Bias Correction in Fincha Watershed. *Am. J. Agric. Environ. Sci.* **2018**, *18*, 324–337. [[CrossRef](#)]
53. Arsano, Y. *Ethiopia and the Nile Dilemmas of National and Regional Hydropolitics*; Center for Security Studies, Swiss Federal Institute of Technology: Zurich, Switzerland, 2007.
54. Dibaba, W.T.; Miegel, K.; Demissie, T.A. Evaluation of the CORDEX regional climate models performance in simulating climate conditions of two catchments in Upper Blue Nile Basin. *Dyn. Atmos. Ocean.* **2019**, *87*, 1–14. [[CrossRef](#)]
55. FAO Major Soils of the World. *Land and Water Digital Media Series 19*; FAO: Rome, Italy, 2002.
56. Halmy, M.W.A.; Gessler, P.E.; Hicke, J.A.; Salem, B.B. Land use/land cover change detection and prediction in the north-western coastal desert of Egypt using Markov-CA. *Appl. Geogr.* **2015**, *63*, 101–112. [[CrossRef](#)]
57. Scott, B.W.A. Reliability of Content Analysis: The Case of Nominal Scale Coding. *Public Opin. Q.* **1955**, *19*, 321–325. [[CrossRef](#)]
58. Rathjens, H.; Bieger, K.; Srinivasan, R.; Chaubey, I.; Arnold, J.G. CMhyd User Manual. 2016. Available online: <http://swat.tamu.edu/software/cmhyd/> (accessed on 2 January 2020).
59. Teutschbein, C.; Seibert, J. Bias correction of regional climate model simulations for hydrological climate-change impact studies: Review and evaluation of different methods. *J. Hydrol.* **2012**, *456–457*, 12–29. [[CrossRef](#)]
60. Luo, M.; Liu, T.; Meng, F.; Duan, Y.; Frankl, A.; Bao, A.; Maeyer, P. De Comparing Bias Correction Methods Used in Downscaling Precipitation and Temperature from Regional Climate Models: A Case Study from the Kaidu River Basin in Western China. *Water* **2018**, *10*, 1046. [[CrossRef](#)]
61. Zhang, B.; Shrestha, N.K.; Daggupati, P.; Rudra, R.; Shukla, R.; Kaur, B.; Hou, J. Quantifying the Impacts of Climate Change on Streamflow Dynamics of Two Major Rivers of the Northern Lake Erie Basin in Canada. *Sustainability* **2018**, *10*, 2897. [[CrossRef](#)]
62. Arnold, J.G.; Srinivasan, R.; Muttiah, R.S.; Williams, J.R. Large Area Hydrologic Modeling and Assessment Part I: Model Development. *J. Am. Water Resour. Assoc.* **1998**, *34*, 73–89. [[CrossRef](#)]
63. Neitsch, S.L.; Arnold, J.G.; Kiniry, J.R.; Williams, J.R. *Soil & Water Assessment Tool Theoretical Documentation Version 2009*; Texas Water Resources Institute Technical Report No.406; Texas A&M University System: College Station, TX, USA, 2011; Available online: <https://swat.tamu.edu/media/99192/swat2009-theory.pdf> (accessed on 23 February 2020).
64. Abbaspour, K.C. *SWAT-CUP: SWAT Calibration and Uncertainty Programs—A User Manual*; Eawag: Dübendorf, Switzerland, 2015.

65. Moriasi, D.N.; Arnold, J.G.; Van Liew, M.W.; Bingner, R.L.; Harmel, R.D.; Veith, T.L. Model evaluation guidelines for systematic quantification of accuracy in watershed simulation. *Am. Soc. Agric. Biol. Eng.* **2007**, *50*, 885–900.
66. Abbaspour, K.C.; Rouholahnejad, E.; Vaghefi, S.; Srinivasan, R.; Yang, H.; Kløve, B. A continental-scale hydrology and water quality model for Europe: Calibration and uncertainty of a high-resolution large-scale SWAT model. *J. Hydrol.* **2015**, *524*, 733–752. [[CrossRef](#)]
67. Ayele, G.T.; Teshale, E.Z.; Yu, B.; Rutherford, I.D.; Jeong, J. Streamflow and Sediment Yield Prediction for Watershed Prioritization in the Upper Blue Nile. *Water* **2017**, *9*, 782. [[CrossRef](#)]
68. Seleshi, Y.; Camberlin, P. Recent changes in dry spell and extreme rainfall events in Ethiopia. *Theor. Appl. Clim.* **2006**, *83*, 181–191. [[CrossRef](#)]
69. de Hipt, F.O.; Diekkrügera, B.; Steupa, G.; Yiraa, Y.; Hoffmannb, T.; Rode, M. Modeling the impact of climate change on water resources and soil erosion in a tropical catchment in Burkina Faso, West Africa. *Catena* **2018**, *163*, 63–77. [[CrossRef](#)]
70. Girma, M.M. *Potential Impact of Climate and Land Use Changes on the Water Resources of the Upper Blue Nile Basin*; Freie Universität: Berlin, Germany, 2012.
71. GFDRR. *Climate Risk and Adaptation Country Profile: Ethiopia*; World Bank: Washington, DC, USA, 2011.
72. Woldesenbet, T.A.; Elagib, N.A.; Ribbe, L.; Heinrich, J. Catchment response to climate and land use changes in the Upper Blue Nile Sub-Basins, Ethiopia. *Sci. Total Environ.* **2018**, *644*, 193–206. [[CrossRef](#)]
73. Shi, P.; Ma, X.; Hou, Y.; Li, Q. Effects of Land-Use and Climate Change on Hydrological Processes in the Upstream of Huai River, China. *Water Resour. Manag.* **2013**, *27*, 1263–1278. [[CrossRef](#)]
74. Gashaw, T.; Tulu, T.; Argaw, M.; Worqlul, A.W. Modeling the hydrological impacts of land use/land cover changes in the Andassa watershed, Blue Nile Basin, Ethiopia. *Sci. Total Environ.* **2018**, *619–620*, 1394–1408. [[CrossRef](#)] [[PubMed](#)]
75. Coffel, E.D.; Keith, B.; Lesk, C.; Horton, R.M.; Bower, E.; Lee, J.; Mankin, J.S. Future Hot and Dry Years Worsen Nile Basin Water Scarcity Despite Projected Precipitation Increases. *Earth's Future* **2019**, *7*. [[CrossRef](#)]
76. Serdeczny, O.; Adams, S.; Coumou, D.; Hare, W.; Perrette, M. Climate change impacts in Sub-Saharan Africa: From physical changes to their social repercussions. *Reg. Environ. Chang.* **2016**, 1–16. [[CrossRef](#)]
77. Gebremeskel, G.; Kebede, A. Estimating the effect of climate change on water resources: Integrated use of climate and hydrological models in the Werii watershed of the Tekeze river basin, Northern Ethiopia. *Agric. Nat. Resour.* **2018**, *52*, 195–207. [[CrossRef](#)]
78. Phung, Q.A.; Thompson, A.L.; Baffaut, C.; Costello, C.; Sadler, E.J.; Svoma, B.M.; Lupo, A.; Gautam, S. Climate and Land Use Effects on Hydrologic Processes in a Primarily Rain-Fed, Agricultural Watershed. *J. Am. Water Resour. Assoc.* **2019**, *55*, 1196–1215. [[CrossRef](#)]
79. Kim, J.; Choi, J.; Choi, C.; Park, S. Impacts of changes in climate and land use/land cover under IPCC RCP scenarios on streamflow in the Hoeya River Basin, Korea. *Sci. Total Environ.* **2013**, *452–453*, 181–195. [[CrossRef](#)]

